

A new approach for designing dynamic balanced serial mechanisms

André Garnier Coutinho ^a, Tarcisio Antonio Hess Coelho ^b

^a *Department of Mechatronics and Mechanical Systems Engineering, Escola Politecnica, University of Sao Paulo, Brazil. E-mail: andre.garnier.coutinho@usp.br*

^b *Department of Mechatronics and Mechanical Systems Engineering, Escola Politecnica, University of Sao Paulo, Brazil. E-mail: tarchess@usp.br*

Abstract

Adaptive balancing means that the mechanical structure of the manipulator is modified in order to achieve the decoupling of dynamic equations. This work deals with a systematic methodology for the adaptive balancing. Basically, two balancing techniques are employed here: the addition of counterweight and counter-rotating disks coupled to the moving links. In addition, the feasibility of the dynamic decoupling for 3 distinct types of serial manipulators is discussed regarding the achievement of such balancing and the complexity level of the modified mechanical structure. The balancing conditions are developed for 3-dof spatial and planar open loop-kinematic chain mechanisms, whose topologies are composed of revolute and prismatic joints.

KEYWORDS: Dynamic balancing, serial mechanisms

Nomenclature

a, b, \dots	Scalars, components of column-matrices, components of matrices or indexes
A, B, \dots	Scalars, components of column-matrices or components of matrices
$\mathbf{a}, \mathbf{b}, \dots$	Column-matrices
$\mathbb{A}, \mathbb{B}, \dots$	Matrices
$\mathbf{a}, \mathbf{b}, \dots$	Vectors
$\mathbf{A}, \mathbf{B}, \dots$	Coordinate systems
$\mathcal{A}, \mathcal{B}, \dots$	Sets or multibody mechanical systems*
\mathbf{B}_i	Coordinate system fixed in the i^{th} rigid body of the mechanical system
\mathbb{C}	Kinematic constraints matrix
$c(.)$	Shorthand notation for $\cos(.)$
g	gravitational acceleration
$\mathbf{g}^{\#}$	Generalized gravitational forces column-matrix of a serial mechanism
$\mathbf{g}_i^{\#}$	Generalized gravitational forces column-matrix of a counter-rotating disc
\mathbf{g}'	Generalized uncoupled gravitational forces column-matrix of a serial mechanism coupled with counter-rotating discs

*A multibody mechanical system will be conceived as a set whose elements are material bodies, joints, actuators, energy storage, dissipation and transformation elements and a mathematical model (which includes physical parameters, model variables and constitutive, constraint and dynamic equations).

$\mathbf{g}^\#$	Generalized gravitational forces column-matrix of a serial mechanism coupled with counter-rotating discs
$J_{x_i}, J_{y_i}, J_{z_i}$	Moments of inertia of the i^{th} rigid body of the mechanical system
l_i	Length of the i^{th} bar of a serial mechanism
l_{g_i}	Position of the mass center of the i^{th} bar relative to the i^{th} joint and of a serial mechanism
m_i	Mass of the i^{th} rigid body of the mechanical system
$\mathbb{M}^\#$	Generalized inertia matrix of a serial mechanism
$\mathbb{M}_i^\#$	Generalized inertia matrix of a counter-rotating disc
\mathbb{M}'	Generalized uncoupled inertia matrix of a serial mechanism coupled with counter-rotating discs
$\mathbb{M}'^\#$	Generalized inertia matrix of a serial mechanism coupled with counter-rotating discs
\mathcal{N}	Inertial reference frame
$\mathbb{p}^\#$	Independent quasi-velocities column-matrix
\mathbb{p}°	Redundant quasi-velocities column-matrix
\mathbb{p}	Quasi-velocities column-matrix
q_i	Generalized coordinate
$\mathbf{q}^\#$	Independent generalized coordinates column-matrix
$s(\cdot)$	Shorthand notation for $\sin(\cdot)$
u_i	Effort made by the i^{th} actuator of a serial mechanism
\mathbf{u}	Generalized actuators' efforts column-matrix
$\mathbf{v}^\#$	Generalized coupled gyroscopic inertia forces column-matrix of a serial mechanism
$\mathbf{v}_i^\#$	Generalized coupled gyroscopic inertia forces column-matrix of a counter-rotating disc
\mathbf{v}'	Generalized uncoupled gyroscopic inertia forces column-matrix of a serial mechanism coupled with counter-rotating discs
$\mathbf{v}'^\#$	Generalized coupled gyroscopic inertia forces column-matrix of a of a serial mechanism coupled with counter-rotating discs
$[\boldsymbol{\omega}_i]_{\mathcal{B}_j}$	Angular velocity of the i^{th} rigid body of the mechanical system measured relatively to a inertial reference frame \mathcal{N} , written in the basis of \mathcal{B}_j
ω_{x_i}	1 st component of $[\boldsymbol{\omega}_i]_{\mathcal{B}_i}$
ω_{y_i}	2 nd component of $[\boldsymbol{\omega}_i]_{\mathcal{B}_i}$
ω_{z_i}	3 rd component of $[\boldsymbol{\omega}_i]_{\mathcal{B}_i}$
$\mathbf{0}$	Null column-matrix or null matrix
$\mathbb{1}$	Identity matrix
$[\mathbb{1}]_{\mathcal{B}_i \mathcal{B}_j}$	Change of basis matrix, i.e. $[\mathbf{v}]_{\mathcal{B}_i} = [\mathbb{1}]_{\mathcal{B}_i \mathcal{B}_j} \cdot [\mathbf{v}]_{\mathcal{B}_j}$
$[\cdot]^\top$	Matrix transposition

1 Introduction and literature review

Balancing is an important issue related to the design of mechanical systems in general, and also serial manipulators, in particular. In fact, the performance of serial mechanisms associated to specific applications depends on the choice of the balancing method, namely, either static or dynamic, either passive or active, whether it is valid for a given trajectory or even for any motion.

Adaptive balancing means that the mechanical structure of the manipulator is modified in order to achieve the decoupling of dynamic equations. The modifications comprise the addition of either counterweights, or counter-rotating disks or even both to the original kinematic chain of the manipulator. Consequently, the terms associated to gravitational, centripetal and Coriolis efforts are completely eliminated from the dynamic equations. As a matter of fact, the effective inertias for all the actuator axes are constant and the mathematical expressions of the driving torques/forces become rather simple. One of the main advantages of this approach concerns the reduction of computing time for a closed-loop control of manipulators. Such reduction is really significant and it constitutes in a great benefit for real-time applications.

In a statically balanced mechanism, the potential energy is invariant. Hence, the actuator torques/forces are null at any configuration [6].

On the other hand, in a dynamically balanced mechanism, the shaking forces and shaking moments at its frame are reduced or even eliminated. As a consequence, the mechanism components are less susceptible to vibration, wear and fatigue [4], improving its life.

Passive balancing means that the original mechanism architecture is modified by using some techniques. The most common techniques are the addition of counterweights [1, 2, 3, 4, 6, 7, 12, 15, 16], the use of counter-rotating inertias [2, 4, 15, 16] and the redistribution of masses [8, 9]. Alternatively, other works propose the addition of extra links [5, 12, 13]. However, for high speed manipulators, these techniques might cause the increase of the actuator torques and the size of links and joints.

Hence, in order to avoid such undesirable effects, some authors [6, 7, 8, 9, 10, 13] recommend the use of elastic springs attached to the mechanism.

For the active balancing [2, 3, 11, 14, 15, 16], more complex modifications are needed to implement it. For instance, the counterweights position in the moving links might be altered according to the end-effector load or the given trajectory. Hence, additional actuators/sensors and control are usually employed to reach satisfactory performance levels. Arakelian and Smith [2] employ a computer control of the motion of a inertia flywheel connected to the mechanism. Moreover, Coelho et al. [15], Moradi et al. [16] and [17] use the adaptive balancing to achieve the decoupling of dynamic equations for open-loop kinematic chain mechanisms. Consequently, this action simplifies the control of manipulators due to the fact that the actuators can be controlled independently.

The contributions of this work are the following: to present a systematic methodology for the adaptive balancing, to discuss the feasibility of the dynamic decoupling for 3 distinct types of serial manipulators, not only in terms of the possibility to achieve such balancing but also in terms of the increase in the complexity level of the modified mechanical structure. The analysed manipulators correspond to 3-dof spatial and planar open loop-kinematic chain, whose topologies are composed of revolute and prismatic joints.

This work is organized as follows. Section 2 describes the proposed methodology, while section 3 deals with the application of the methodology to 3 types of serial manipulators. Finally, the conclusions are drawn in section 4.

2 Methodology

2.1 Dynamic Model

O modelo dinâmico de um mecanismo serial pode ser escrito da seguinte maneira:

$$\mathbb{M}^{\#}(\mathbf{q}^{\#})\ddot{\mathbf{q}}^{\#} + \mathbf{v}^{\#}(\mathbf{q}^{\#}, \dot{\mathbf{q}}^{\#}) + \mathbf{g}^{\#}(\mathbf{q}^{\#}) = \mathbf{u} \quad (1)$$

Sendo $\mathbf{q}^{\#}$ um conjunto de coordenadas generalizadas independentes, cujos elementos são os deslocamentos relativos das juntas e \mathbf{u} os esforços generalizados nas direções das quasi-velocidades independentes

$$\mathbb{p}^\# = \dot{\mathbf{q}}^\#.$$

Para realizar o balanceamento dinâmico de um mecanismo serial, utilizando abordagem proposta, é necessário primeiro obter o modelo do mecanismo desbalanceado. Como em um mecanismo serial é possível de expressar todas as velocidades lineares absolutas dos centros de massa das barras e todas as velocidades angulares absolutas das barras em função de $\mathbf{q}^\#$ e $\dot{\mathbf{q}}^\#$, o modelo dinâmico pode ser obtido sem grandes dificuldades utilizando métodos de mecânica analítica, como Lagrange, Kane e Orsino, aliados a programas ou bibliotecas de linguagens de programação que são capazes de utilizar manipulação simbólica, como o Mathematica e o SymPy.

2.2 Static Balancing

Depois de obtido o modelo dinâmico, realiza-se o balanceamento estático encontrando as posições dos centros de massa das barras que fazem com que $\mathfrak{g}^\# = \mathbf{0}$. Isso é possível para mecanismos com juntas apenas rotativas e mecanismos com juntas prismáticas cujas direções são ortogonais à gravidade. O posicionamento dos centros de massa é realizado mecanicamente com o prologamento das barras do mecanismo e adição de contra-pesos.

2.3 Dynamic Balancing

O balanceamento dinâmico é obtido acoplando discos girantes ao modelo do mecanismo estáticamente balanceado. Isso é feito utilizando a técnica de acoplamento de subsistemas do Método Orsino.

Seja \mathcal{M}_0 um subsistema mecânico constituído por um mecanismo serial estaticamente balanceado, cuja equação de movimento é dada pela equação (1), com $\mathfrak{g}^\# = \mathbf{0}$. Seja \mathcal{M}_i um subsistema mecânico constituído de um disco girante que será acoplado ao mecanismo, cuja equação de movimento é dada por:

$$\mathbb{M}_i^\# \dot{\mathbf{p}}^\# + \mathbf{v}_i^\# + \mathfrak{g}_i^\# = \mathbf{u}_i \quad (2)$$

Sendo $\mathbf{p}^\#$ um conjunto de quasi-velocidades independentes, cujos elementos são as componentes não nulas do vetor velocidade angular absoluta do disco, escrito em uma base solidária ao disco, e $\mathbf{v}_i^\# = \mathfrak{g}_i^\# = \mathbf{u}_i = \mathbf{0}$. Nesse modelo, são considerados apenas os efeitos das inércias rotativas, sendo os efeitos da massa do disco considerados na massa e nos momentos de inércia da barra em que o disco for acoplado, efetuando também no cálculo do posicionamento dos contra-pesos, de modo que o mecanismo continue estáticamente balanceado.

Supondo que irão ser acoplados n discos ao mecanismo, são feitas as seguintes definições:

$$\mathbb{M}' = \begin{bmatrix} \mathbb{M}^\# & \mathbf{0} & \dots & \mathbf{0} \\ \mathbf{0} & \mathbb{M}_1^\# & \dots & \mathbf{0} \\ \vdots & \vdots & \ddots & \vdots \\ \mathbf{0} & \mathbf{0} & \dots & \mathbb{M}_n^\# \end{bmatrix} \quad (3)$$

$$\mathbf{v}' = \begin{bmatrix} \mathbf{v}^{\#T} & \mathbf{v}_1^{\#T} & \dots & \mathbf{v}_n^{\#T} \end{bmatrix}^T \quad (4)$$

$$\mathfrak{g}' = \begin{bmatrix} \mathfrak{g}^{\#T} & \mathfrak{g}_1^{\#T} & \dots & \mathfrak{g}_n^{\#T} \end{bmatrix}^T \quad (5)$$

$$\mathbf{p}^\circ = \begin{bmatrix} \mathbf{p}_1^{\#T} & \dots & \mathbf{p}_n^{\#T} \end{bmatrix}^T \quad (6)$$

$$\mathbf{p} = \begin{bmatrix} \mathbf{p}^{\#T} & \mathbf{p}^{\circ T} \end{bmatrix}^T \quad (7)$$

Seja \underline{p}° o vetor p° escrito em função de $q^\#$ e $p^\#$, ou seja:

$$p^\circ = \underline{p}^\circ(q^\#, p^\#) \quad (8)$$

Definimos a seguinte matriz das restrições cinemáticas:

$$\mathbb{C} = \begin{bmatrix} \underline{1} \\ \frac{\partial \underline{p}^\circ}{\partial p^\#} \end{bmatrix} \quad (9)$$

O modelo dinâmico do mecanismo serial com os discos acoplados, é dado por:

$$\mathbb{M}'^\#(q^\#)\ddot{q}^\# + v'^\#(q^\#, \dot{q}^\#) + g'^\#(q^\#) = u \quad (10)$$

Sendo:

$$\mathbb{M}'^\# = \mathbb{C}^\top \mathbb{M}' \mathbb{C} \quad (11)$$

$$v'^\# = \mathbb{C}^\top (\mathbb{M}' \dot{\mathbb{C}} \dot{q}^\# + v') \quad (12)$$

$$g'^\# = \mathbb{C}^\top g' \quad (13)$$

O balanceamento dinâmico é obtido encontrando as relações entre os parâmetros do sistema que tornam a matriz $\mathbb{M}'^\#$ diagonal e o vetor $v'^\#$ nulo.

3 Applying the technique

Nesta seção, a metodologia proposta será aplicada em três diferentes mecanismos seriais de 3 graus de liberdade, um plano e dois espaciais. Para isso, primeiramente faremos algumas definições válidas para os mecanismos em questão:

$$\mathbb{M}^\# = \begin{bmatrix} D_{11} & D_{12} & D_{13} \\ D_{12} & D_{22} & D_{23} \\ D_{13} & D_{23} & D_{33} \end{bmatrix} \quad (14)$$

$$v^\# = \begin{bmatrix} D_{111} & D_{122} & D_{133} \\ D_{211} & D_{222} & D_{233} \\ D_{311} & D_{322} & D_{333} \end{bmatrix} \begin{bmatrix} \dot{q}_1^2 \\ \dot{q}_2^2 \\ \dot{q}_3^2 \end{bmatrix} + 2 \begin{bmatrix} D_{112} & D_{113} & D_{123} \\ D_{212} & D_{213} & D_{223} \\ D_{312} & D_{313} & D_{323} \end{bmatrix} \begin{bmatrix} \dot{q}_1 \dot{q}_2 \\ \dot{q}_1 \dot{q}_3 \\ \dot{q}_2 \dot{q}_3 \end{bmatrix} \quad (15)$$

$$g^\# = [D_1 \quad D_2 \quad D_3]^\top \quad (16)$$

$$q^\# = [q_1 \quad q_2 \quad q_3]^\top \quad (17)$$

$$u = [u_1 \quad u_2 \quad u_3]^\top \quad (18)$$

Para juntas rotativas definimos $q_i = \theta_i$ e $u_i = \tau_i$, e para juntas prismáticas definimos $q_i = d_i$ and $u_i = f_i$, para ficar de acordo com as notações mais tradicionais dessa área.

3.1 3-DOF RRR planar serial mechanism

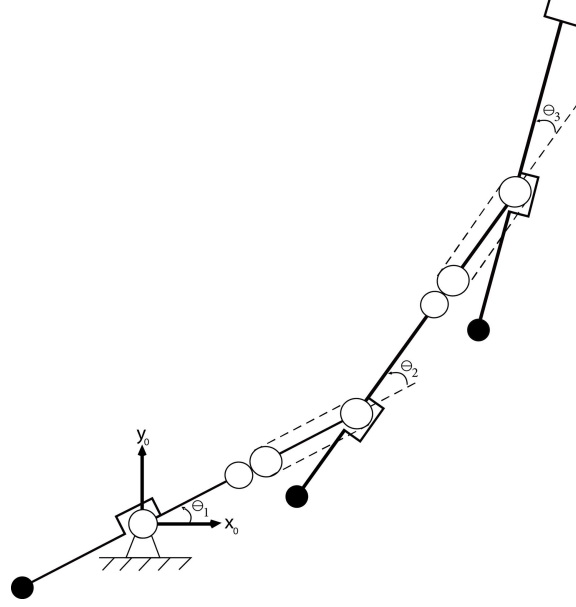


Figure 1: Mecanismo RRR plano balanceado dinamicamente

As componentes de $\mathbf{g}^\#$ para o mecanismo em questão desbalanceado são dadas por:

$$\begin{cases} D_1 = g[(m_1 l_{g1} + m_2 l_1 + m_3 l_1) \cos(\theta_1) + (m_2 l_{g2} + m_3 l_2) \cos(\theta_1 + \theta_2) + m_3 l_{g3} \cos(\theta_1 + \theta_2 + \theta_3)] \\ D_2 = g[(m_2 l_{g2} + m_3 l_2) \cos(\theta_1 + \theta_2) + m_3 l_{g3} \cos(\theta_1 + \theta_2 + \theta_3)] \\ D_3 = g[m_3 l_{g3} \cos(\theta_1 + \theta_2 + \theta_3)] \end{cases} \quad (19)$$

Realizando o balanceamento estático, temos:

$$\begin{cases} D_1 = 0 \\ D_2 = 0 \\ D_3 = 0 \end{cases} \Rightarrow \begin{cases} l_{g1} = -\frac{l_1(m_2 + m_3)}{m_1} \\ l_{g2} = -\frac{l_2 m_3}{m_2} \\ l_{g3} = 0 \end{cases} \quad (20)$$

Substituindo (20) no modelo do mecanismo, obtemos o modelo dinâmico do mecanismo estaticamente balanceado:

$$\begin{cases} D_{11} = J_{z1} + J_{z2} + J_{z3} + m_2 l_1^2 + m_3 (l_1^2 + l_2^2) + \frac{l_1^2 (m_2 + m_3)^2}{m_1} + \frac{l_2^2 m_3^2}{m_2} \\ D_{22} = J_{z2} + J_{z3} + m_3 l_2^2 + \frac{l_2^2 m_3^2}{m_2} \\ D_{33} = J_{z3} \\ D_{12} = D_{22} \\ D_{13} = D_{23} = D_{33} \\ \mathbf{v}^\# = \mathbf{0} \\ \mathbf{g}^\# = \mathbf{0} \end{cases} \quad (21)$$

Para realizar o balanceamento dinâmico, acoplamos 4 discos ao mecanismo, assim como é mostrado na figura 1. Como os discos giram em apenas um plano, utilizamos os seguintes modelos dinâmicos para eles:

$$\mathbb{M}_i^\# = [J_{z_{i+3}}]; \quad \mathbb{P}_i^\# = [\omega_{z_{i+3}}], \quad i = 1, 2, 3, 4 \quad (22)$$

Os discos 1 e 2 estão acoplados à barra 1, sendo que o disco 1 apresenta um giro de θ_2 relativo à barra 1, devido à transmissão por correia do giro do motor 2, enquanto o disco 2 apresenta um giro de $\beta\theta_2$, com $\beta < 0$, relativo à barra 1, devido à transmissão por engrenagem do giro do disco 1.

Os discos 3 e 4 estão acoplados à barra 2, sendo que o disco 3 apresenta um giro de θ_3 relativo à barra 2, devido à transmissão por correia do giro do motor 3, enquanto o disco 4 apresenta um giro de $\gamma\theta_3$, com $\gamma < 0$, relativo à barra 2, devido à transmissão por engrenagem do giro do disco 3.

Sendo assim, obtemos os seguintes vínculos de quasi-velocidades:

$$\begin{cases} \omega_{z_4} = \omega_{z_1} + \dot{\theta}_2 \\ \omega_{z_5} = \omega_{z_1} + \beta\dot{\theta}_2 \\ \omega_{z_6} = \omega_{z_2} + \dot{\theta}_3 \\ \omega_{z_7} = \omega_{z_2} + \gamma\dot{\theta}_3 \end{cases} \Rightarrow \begin{cases} \omega_{z_4} = \dot{\theta}_1 + \dot{\theta}_2 \\ \omega_{z_5} = \dot{\theta}_1 + \beta\dot{\theta}_2 \\ \omega_{z_6} = \dot{\theta}_1 + \dot{\theta}_2 + \dot{\theta}_3 \\ \omega_{z_7} = \dot{\theta}_1 + \dot{\theta}_2 + \gamma\dot{\theta}_3 \end{cases} \Rightarrow \underline{\mathbb{P}}^\circ = \begin{bmatrix} \dot{\theta}_1 + \dot{\theta}_2 \\ \dot{\theta}_1 + \beta\dot{\theta}_2 \\ \dot{\theta}_1 + \dot{\theta}_2 + \dot{\theta}_3 \\ \dot{\theta}_1 + \dot{\theta}_2 + \gamma\dot{\theta}_3 \end{bmatrix} \quad (23)$$

$$\therefore \mathbb{C} = \begin{bmatrix} \mathbb{1} \\ \frac{\partial \underline{\mathbb{P}}^\circ}{\partial \underline{\mathbb{P}}^\#} \end{bmatrix} = \begin{bmatrix} 1 & 0 & 0 \\ 0 & 1 & 0 \\ 0 & 0 & 1 \\ 1 & 1 & 0 \\ 1 & \beta & 0 \\ 1 & 1 & 1 \\ 1 & 1 & \gamma \end{bmatrix} \quad (24)$$

Aplicando (21), (22) e (24) em (11), (12) e (13), obtemos o modelo do mecanismo estaticamente balanceado com os discos acoplados:

$$\begin{cases} D'_{11} = D_{11} + J_{z_4} + J_{z_5} + J_{z_6} + J_{z_7} \\ D'_{22} = D_{22} + J_{z_4} + J_{z_5}\beta^2 + J_{z_6} + J_{z_7} \\ D'_{33} = D_{33} + J_{z_6} + J_{z_7}\gamma^2 \\ D'_{12} = D_{12} + J_{z_4} + J_{z_5}\beta + J_{z_6} + J_{z_7} \\ D'_{13} = D_{13} + J_{z_6} + J_{z_7}\gamma \\ D'_{23} = D'_{13} \\ \mathbb{V}^\# = 0 \end{cases} \quad (25)$$

Para realizar o balanceamento dinâmico, encontramos os valores de β e γ em função dos parâmetros do mecanismo que tornam a matriz $\mathbb{M}^\#$ diagonal. Assim, temos:

$$\begin{cases} D'_{12} = 0 \\ D'_{13} = 0 \end{cases} \Rightarrow \begin{cases} \beta = -\frac{J_{z_2} + J_{z_3} + J_{z_4} + J_{z_6} + J_{z_7} + m_3 l_2^2 + \frac{m_3^2 l_2^2}{m_2}}{J_{z_5}} \\ \gamma = -\frac{J_{z_3} + J_{z_6}}{J_{z_7}} \end{cases} \quad (26)$$

Substituindo (26) em (25), obtemos o modelo do mecanismo dinamicamente balanceado:

$$\begin{cases} \tau_1 = k_1 \ddot{\theta}_1 \\ \tau_2 = k_2 \ddot{\theta}_2 \\ \tau_3 = k_3 \ddot{\theta}_3 \end{cases} \quad (27)$$

Sendo:

$$\begin{cases} k_1 = J_{z_1} + J_{z_2} + J_{z_3} + J_{z_4} + J_{z_5} + J_{z_6} + J_{z_7} + m_2 l_1^2 + m_3 (l_1^2 + l_2^2) + \frac{l_1^2 (m_2 + m_3)^2}{m_1} + \frac{l_2^2 m_3^2}{m_2} \\ k_2 = J_{z_2} + J_{z_3} + J_{z_4} + J_{z_6} + J_{z_7} + m_3 l_2^2 + \frac{l_2^2 m_3^2}{m_2} + \frac{(J_{z_2} + J_{z_3} + J_{z_4} + J_{z_6} + J_{z_7} + m_3 l_2^2 + \frac{m_3^2 l_2^2}{m_2})^2}{J_{z_5}} \\ k_3 = \frac{(J_{z_3} + J_{z_6})(J_{z_3} + J_{z_6} + J_{z_7})}{J_{z_7}} \end{cases} \quad (28)$$

3.2 3-DOF RRR spatial serial mechanism

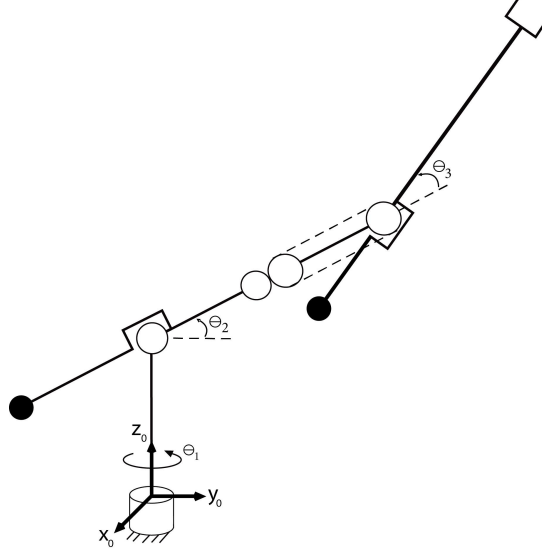


Figure 2: Mecanismo RRR espacial balanceado dinamicamente

As componentes de $\mathfrak{g}^\#$ para o mecanismo em questão desbalanceado são dadas por:

$$\begin{cases} D_1 = 0 \\ D_2 = g[(m_2 l_{g_2} + m_3 l_2) \mathbf{c}(\theta_2) + m_3 l_{g_3} \mathbf{c}(\theta_2 + \theta_3)] \\ D_3 = g[m_3 l_{g_3} \mathbf{c}(\theta_2 + \theta_3)] \end{cases} \quad (29)$$

Realizando o balanceamento estático, temos:

$$\begin{cases} D_2 = 0 \\ D_3 = 0 \end{cases} \Rightarrow \begin{cases} l_{g_2} = -\frac{l_2 m_3}{m_2} \\ l_{g_3} = 0 \end{cases} \quad (30)$$

Substituindo (30) no modelo do mecanismo, obtemos o modelo dinâmico do mecanismo estaticamente balanceado:

$$\begin{cases} D_{11} = J_{x_2} \mathbf{s}^2(\theta_2) + J_{x_3} \mathbf{s}^2(\theta_2 + \theta_3) + J_{z_1} + J_{y_2} \mathbf{c}^2(\theta_2) + J_{y_3} \mathbf{c}^2(\theta_2 + \theta_3) + m_3 (l_1 + l_2 \mathbf{c}(\theta_2))^2 + \frac{(m_2 l_1 - m_3 l_2 \mathbf{c}(\theta_2))^2}{m_2} \\ D_{22} = J_{z_2} + J_{z_3} + m_2 l_2^2 + \frac{l_2^2 m_3^2}{m_2} \\ D_{33} = J_{z_3} \\ D_{12} = D_{13} = 0 \\ D_{23} = D_{33} \\ D_{211} = -\frac{1}{2} \left((J_{x_2} - J_{y_2}) \mathbf{s}(2\theta_2) + (J_{x_3} - J_{y_3} - m_3 l_2^2 (1 + \frac{m_3}{m_2})) \mathbf{s}(2\theta_2 + 2\theta_3) \right) \\ D_{311} = \frac{1}{2} \left((J_{y_3} - J_{x_3}) \mathbf{s}(2\theta_2 + 2\theta_3) \right) \\ D_{111} = D_{122} = D_{133} = D_{222} = D_{233} = D_{322} = D_{333} = 0 \\ D_{112} = -D_{211} \\ D_{113} = -D_{311} \\ D_{123} = D_{212} = D_{213} = D_{223} = D_{312} = D_{313} = D_{323} = 0 \\ \mathfrak{g} = 0 \end{cases} \quad (31)$$

Para realizar o balanceamento dinâmico, acoplamos 2 discos ao mecanismo, assim como é mostrado na figura 2. Utilizamos os seguintes modelos dinâmicos para eles:

$$\mathbb{M}_i^\# = \begin{bmatrix} J_{x_{i+3}} & 0 & 0 \\ 0 & J_{y_{i+3}} & 0 \\ 0 & 0 & J_{z_{i+3}} \end{bmatrix}; \quad \mathbb{P}_i^\# = \begin{bmatrix} \omega_{x_{i+3}} \\ \omega_{y_{i+3}} \\ \omega_{z_{i+3}} \end{bmatrix}, \quad i = 1, 2 \quad (32)$$

Os discos 1 e 2 estão acoplados à barra 2, sendo que o disco 1 apresenta um giro de θ_3 relativo à barra 2, devido à transmissão por correia do giro do motor 3, enquanto o disco 2 apresenta um giro de $\beta\theta_3$, com $\beta < 0$, relativo à barra 2, devido à transmissão por engrenagem do giro do disco 2.

Sendo assim, obtemos os seguintes vínculos de quasi-velocidades:

$$\begin{cases} [\omega_4]_{B_4} = [\mathbb{1}]_{B_4 | B_2} [\omega_2]_{B_2} + \begin{bmatrix} 0 \\ 0 \\ \dot{\theta}_3 \end{bmatrix} \\ [\omega_5]_{B_5} = [\mathbb{1}]_{B_5 | B_2} [\omega_2]_{B_2} + \begin{bmatrix} 0 \\ 0 \\ \beta\dot{\theta}_3 \end{bmatrix} \end{cases} \Rightarrow \begin{cases} \omega_{x_4} = (\dot{\theta}_1 s(\theta_2))c(\theta_3) + (\dot{\theta}_1 c(\theta_2))s(\theta_3) \\ \omega_{y_4} = -(\dot{\theta}_1 s(\theta_2))s(\theta_3) + (\dot{\theta}_1 c(\theta_2))c(\theta_3) \\ \omega_{z_4} = \dot{\theta}_2 + \dot{\theta}_3 \\ \omega_{x_5} = (\dot{\theta}_1 s(\theta_2))c(\beta\theta_3) + (\dot{\theta}_1 c(\theta_2))s(\beta\theta_3) \\ \omega_{y_5} = -(\dot{\theta}_1 s(\theta_2))s(\beta\theta_3) + (\dot{\theta}_1 c(\theta_2))c(\beta\theta_3) \\ \omega_{z_5} = \dot{\theta}_2 + \beta\dot{\theta}_3 \end{cases} \quad (33)$$

$$\Rightarrow \underline{\mathbb{P}}^\circ = \begin{bmatrix} \dot{\theta}_1 s(\theta_2 + \theta_3) \\ \dot{\theta}_1 c(\theta_2 + \theta_3) \\ \dot{\theta}_2 + \dot{\theta}_3 \\ \dot{\theta}_1 s(\theta_2 + \beta\theta_3) \\ \dot{\theta}_1 c(\theta_2 + \beta\theta_3) \\ \dot{\theta}_2 + \beta\dot{\theta}_3 \end{bmatrix} \quad (34)$$

$$\mathbb{C} = \begin{bmatrix} \mathbb{1} \\ \frac{\partial \underline{\mathbb{P}}^\circ}{\partial \underline{\mathbb{P}}^\#} \end{bmatrix} = \begin{bmatrix} 1 & 0 & 0 \\ 0 & 1 & 0 \\ 0 & 0 & 1 \\ s(\theta_2 + \theta_3) & 0 & 0 \\ c(\theta_2 + \theta_3) & 0 & 0 \\ 0 & 1 & 1 \\ s(\theta_2 + \beta\theta_3) & 0 & 0 \\ c(\theta_2 + \beta\theta_3) & 0 & 0 \\ 0 & 1 & \beta \end{bmatrix} \quad (35)$$

Aplicando (31), (32) e (35) em (11), (12) e (13), obtemos o modelo do mecanismo estaticamente balanceado com os discos acoplados:

$$\begin{cases} D'_{11} = D_{11} + J_{x_4} s^2(\theta_2 + \theta_2) + J_{x_5} s^2(\beta\theta_2 + \theta_2) + J_{y_4} c^2(\theta_2 + \theta_2) + J_{y_5} c^2(\beta\theta_2 + \theta_2) \\ D'_{22} = D_{22} + J_{z_4} + J_{z_5} \\ D'_{33} = D_{33} + J_{z_4} + J_{z_5} \beta^2 \\ D'_{12} = D'_{13} = 0 \\ D'_{23} = D_{23} + J_{z_4} + J_{z_5} \beta \\ D'_{211} = D_{211} \\ D'_{311} = D_{311} \\ D'_{111} = D'_{122} = D'_{133} = D'_{222} = D'_{233} = D'_{322} = D'_{333} = 0 \\ D'_{112} = D_{112} + \frac{1}{4} \left((J_{x_4} - J_{y_4}) s(2\theta_2 + 2\theta_3) + (J_{x_5} - J_{y_5}) s(2\beta\theta_2 + 2\theta_3) \right) \\ D'_{113} = D_{113} + \frac{1}{4} \left((J_{x_4} - J_{y_4}) s(2\theta_2 + 2\theta_3) + (J_{x_5} - J_{y_5}) s(2\beta\theta_2 + 2\theta_3) \right) \\ D'_{123} = D'_{212} = D'_{213} = D'_{223} = D'_{312} = D'_{313} = D'_{323} = 0 \end{cases} \quad (36)$$

Para realizar o balanceamento dinâmico, encontramos os valores de β em função dos parâmetros do mecanismo que tornam a matriz $\mathbb{M}'^\#$ diagonal e as relações entre os parâmetros do mecanismos que zeram $\mathbb{V}'^\#$. Assim, temos:

$$\begin{cases} D'_{23} = 0 \\ D'_{211} = 0 \\ D'_{311} = 0 \\ D'_{112} = 0 \\ D'_{113} = 0 \end{cases} \Rightarrow \begin{cases} \beta = -\frac{J_{z3}+J_{z4}}{J_{z5}} \\ J_{x2} = J_{y2} \\ J_{x3} = J_{y3} + m_3 l_2^2 (1 + \frac{m_3}{m_2}) \\ J_{x4} = J_{y4} \\ J_{x5} = J_{y5} \end{cases} \quad (37)$$

Substituindo (37) em (36), obtemos o modelo do mecanismo dinamicamente balanceado:

$$\begin{cases} \tau_1 = k_1 \ddot{\theta}_1 \\ \tau_2 = k_2 \ddot{\theta}_2 \\ f_3 = k_3 \ddot{d}_3 \end{cases} \quad (38)$$

Sendo:

$$\begin{cases} k_1 = J_{z1} + J_{y2} + J_{y3} + J_{y4} + J_{y5} + m_2 l_1^2 + m_3 (l_1^2 + l_2^2) + \frac{l_1^2 m_3^2}{m_2} \\ k_2 = J_{z2} + J_{z3} + J_{z4} + J_{z5} + m_3 l_2^2 + \frac{l_1^2 m_3^2}{m_2} \\ k_3 = \frac{(J_{z3}+J_{z4})(J_{z3}+J_{z4}+J_{z5})}{J_{z5}} \end{cases} \quad (39)$$

Repare que as condições necessárias para o balanceamento dinâmico deste mecanismo requerem momentos de inércia transversais muito elevados para as barras 2 e 3, o que não é nada conveniente para um manipulador industrial. O próximo exemplo de aplicação será em outro mecanismo serial espacial de 3 graus de liberdade, em que esse tipo de inconveniente não acontece.

3.3 3-DOF RRP spatial serial mechanism (SCARA)

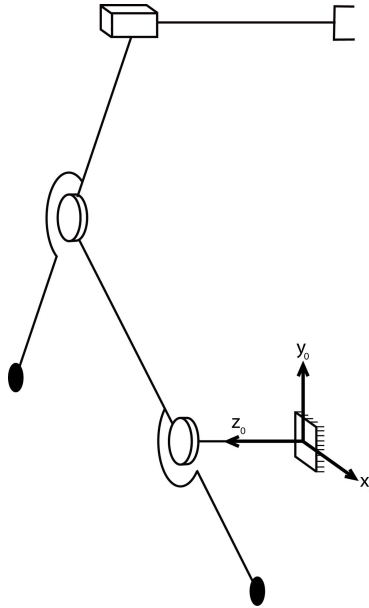


Figure 3: Mecanismo RRP balanceado estaticamente

As componentes de $\mathfrak{g}^\#$ para o mecanismo em questão desbalanceado são dadas por:

$$\begin{cases} D_1 = g[(m_1 l_{g_1} + m_2 l_1 + m_3 l_1) \mathfrak{c}(\theta_1) + m_2 l_{g_2} \mathfrak{c}(\theta_1 + \theta_2)] \\ D_2 = g[m_2 l_{g_2} \mathfrak{c}(\theta_1 + \theta_2)] \\ D_3 = 0 \end{cases} \quad (40)$$

Realizando o balanceamento estático, temos:

$$\begin{cases} D_1 = 0 \\ D_2 = 0 \end{cases} \Rightarrow \begin{cases} l_{g_1} = -\frac{l_1(m_2+m_3)}{m_1} \\ l_{g_2} = 0 \end{cases} \quad (41)$$

Substituindo (41) no modelo do mecanismo, obtemos o modelo dinâmico do mecanismo estaticamente balanceado:

$$\begin{cases} D_{11} = J_{z_1} + J_{z_2} + J_{z_3} + m_2 l_1^2 + m_3 l_1^2 + \frac{l_1^2(m_2+m_3)^2}{m_1} \\ D_{22} = J_{z_2} + J_{z_3} \\ D_{33} = m_3 \\ D_{12} = D_{22} \\ D_{13} = D_{23} = 0 \\ \mathfrak{v}^\# = \mathbb{0} \\ \mathfrak{g}^\# = \mathbb{0} \end{cases} \quad (42)$$

Para realizar o balanceamento dinâmico, acoplamos 2 discos ao mecanismo. Como os discos giram em apenas um plano, utilizamos os seguintes modelos dinâmicos para eles:

$$\mathbb{M}_i^\# = [J_{z_{i+3}}]; \quad \mathbb{P}_i^\# = [\omega_{z_{i+3}}], \quad i = 1, 2 \quad (43)$$

Os discos 1 e 2 estão acoplados à barra 1, sendo que o disco 1 apresenta um giro de θ_2 relativo à barra 1, devido à transmissão por correia do giro do motor 2, enquanto o disco 2 apresenta um giro de $\beta\theta_2$, com $\beta < 0$, relativo à barra 1, devido à transmissão por engrenagem do giro do disco 1.

Sendo assim, obtemos os seguintes vínculos de quasi-velocidades:

$$\begin{cases} \omega_{z_4} = \omega_{z_1} + \dot{\theta}_2 \\ \omega_{z_5} = \omega_{z_1} + \beta\dot{\theta}_2 \end{cases} \Rightarrow \begin{cases} \omega_{z_4} = \dot{\theta}_1 + \dot{\theta}_2 \\ \omega_{z_5} = \dot{\theta}_1 + \beta\dot{\theta}_2 \end{cases} \Rightarrow \overline{\mathbb{P}} = \begin{bmatrix} \dot{\theta}_1 + \dot{\theta}_2 \\ \dot{\theta}_1 + \beta\dot{\theta}_2 \end{bmatrix} \quad (44)$$

$$\mathbb{C} = \begin{bmatrix} \mathbb{1} \\ \frac{\partial \overline{\mathbb{P}}^\circ}{\partial \overline{\mathbb{P}}^\#} \end{bmatrix} = \begin{bmatrix} 1 & 0 & 0 \\ 0 & 1 & 0 \\ 0 & 0 & 1 \\ 1 & 1 & 0 \\ 1 & \beta & 0 \end{bmatrix} \quad (45)$$

Aplicando (42), (43) e (45) em (11), (12) e (13), obtemos o modelo do mecanismo estaticamente balanceado com os discos acoplados:

$$\begin{cases} D'_{11} = D_{11} + J_{z_4} + J_{z_5} \\ D'_{22} = D_{22} + J_{z_4} + J_{z_5} \beta^2 \\ D'_{33} = D_{33} \\ D'_{12} = D_{12} + J_{z_4} + J_{z_5} \beta \\ D'_{13} = 0 \\ D'_{23} = 0 \\ \mathfrak{v}'^\# = \mathbb{0} \end{cases} \quad (46)$$

Para realizar o balanceamento dinâmico, encontramos os valores de β em função dos parâmetros do mecanismo que tornam a matriz $\mathbb{M}'^\#$ diagonal. Assim, temos:

$$D'_{12} = 0 \Rightarrow \beta = -\frac{J_{z_2} + J_{z_3} + J_{z_4}}{J_{z_5}} \quad (47)$$

Substituindo (47) em (46), obtemos o modelo do mecanismo dinamicamente balanceado:

$$\begin{cases} \tau_1 = k_1 \ddot{\theta}_1 \\ \tau_2 = k_2 \ddot{\theta}_2 \\ f_3 = k_3 \ddot{d}_3 \end{cases} \quad (48)$$

Sendo:

$$\begin{cases} k_1 = J_{z_1} + J_{z_2} + J_{z_3} + J_{z_4} + J_{z_5} + m_2 l_1^2 + m_3 l_1^2 + \frac{l_1^2 (m_2 + m_3)^2}{m_1} \\ k_2 = \frac{(J_{z_2} + J_{z_3} + J_{z_4})(J_{z_2} + J_{z_3} + J_{z_4} + J_{z_5})}{J_{z_5}} \\ k_3 = m_3 \end{cases} \quad (49)$$

Repare que as condições necessárias para o balanceamento dinâmico deste mecanismo não requerem restrições nos parâmetros de inércia do mecanismo, como acontece no exemplo anterior. Sendo assim, como o mecanismo do exemplo anterior e o do exemplo em questão são ambos mecanismos seriais espaciais que realizam translações do efetuador em 3 eixos, pode-se dizer que o mecanismo em questão é uma boa alternativa ao mecanismo da seção 3.2 em aplicações em que o balanceamento dinâmico é vantajoso ao sistema.

4 Conclusions

This work dealt with a systematic methodology for the adaptive balancing. Two balancing techniques were employed here: the addition of counterweight and counter-rotating disks coupled to the moving links. In addition, the feasibility of the dynamic decoupling for 3 distinct types of serial manipulators was discussed regarding the achievement of such balancing and the complexity level of the modified mechanical structure. The balancing conditions were developed for 3-dof spatial and planar open loop-kinematic chain mechanisms, whose topologies are composed of revolute and prismatic joints. By analysing the necessary conditions, one can notice that the adaptive balancing brings great benefits for the planar RRR and the spatial RRP. However, for the spatial RRR, in spite of the achievement of the adaptive balancing, the modifications in the mechanical structure cause the increase of the link inertias and the actuator torques, accordingly. Consequently, the authors believe that the discussion provided here might help the designer to choose an adequate topology for a specific application taking advantage of the adaptive balancing whenever it brings no further consequences in terms of the added inertias.

References

- [1] V. Van der Wijk, Shaking moment balancing of mechanisms with principal vectors and moments *Front. Mech. Eng.*, 8(1): 10–16, 2013.
- [2] V. H. Arakelian V. , M. R. Smith, Design of planar 3-dof 3-RRR reactionless parallel manipulators *Mechatronics*, 18: 601–606, 2008.
- [3] J.-T. Seo, J. H. Woo, H. Lim, J. Chung, W. K. Kim, and B.-J. Yi, Design of an Antagonistically Counter-Balancing Parallel Mechanism *IEEE/RSJ International Conference on Intelligent Robots and Systems (IROS)*, Tokyo, November 3-7: 2882–2887, 2013.
- [4] Y. Wu, C. M. Gosselin, Design of reactionless 3-dof and 6-dof parallel manipulators using parallelepiped mechanisms *IEEE Transactions on Robotics*, 21(5): 821–833, 2005.

- [5] C. M. Gosselin, F. Vollmer, G. Ct, Y. Wu, Synthesis and design of reactionless three-degree-of-freedom parallel mechanisms *IEEE Transactions on Robotics and Automation*, 20(2): 191–199, 2004.
- [6] J. Wang, C. M. Gosselin, Static balancing of spatial four-degree-of-freedom parallel mechanisms *Mech. Mach. Theory*, 35: 563–592, 2000.
- [7] J. Wang, C. M. Gosselin, Static balancing of spatial three-degree-of-freedom parallel mechanisms *Mech. Mach. Theory*, 34: 437–452, 1999.
- [8] G. Alici, B. Shirinzadeh, Optimum Force Balancing with Mass Distribution and a Single Elastic Element for a Five-bar Parallel Manipulator *Proceedings of the IEEE International Conference on Robotics and Automation*, Taipei, September 14-19: 3666–3671, 2003.
- [9] G. Alici, B. Shirinzadeh, Optimum dynamic balancing of planar parallel manipulators based on sensitivity analysis *Mech. Mach. Theory*, 41: 1520–1532, 2006.
- [10] M. B. Dehkordi, A. Frisoli, E. Sotgiu, M. Bergamasco, Modelling and Experimental Evaluation of a Static Balancing Technique for a new Horizontally Mounted 3-UPU Parallel Mechanism *International Journal of Advanced Robotic Systems*, 9: 193–205, 2012.
- [11] K. Wang, M. Luo, T. Mei, J. Zhao, Y. Cao, Dynamics Analysis of a Three-DOF Planar Serial-Parallel Mechanism for Active Dynamic Balancing with Respect to a Given Trajectory *International Journal of Advanced Robotic Systems*, 10: 23–33, 2013.
- [12] A. Russo, R. Sinatra, F. Xi, Static balancing of parallel robots *Mech. Mach. Theory*, 40: 191–202, 2005.
- [13] S. K. Agrawal, A. Fattah, Gravity-balancing of spatial robotic manipulators *Mech. Mach. Theory*, 39: 1331–1344, 2004.
- [14] S. Briot, V. Arakelian, J.-P. Le Baron, Shaking force minimization of high-speed robots via centre of mass acceleration control *Mech. Mach. Theory*, 57: 1–12, 2012.
- [15] T. A. H. Coelho, L. Yong, V. F. A. Alves, Decoupling of dynamic equations by means of adaptive balancing of 2-dof open-loop mechanisms *Mech. Mach. Theory*, 39: 871–881, 2004.
- [16] M. Moradi, A. Nikoobin, S. Azadi, Adaptive Decoupling for Open Chain Planar Robots *Transaction B: Mechanical Engineering*, 17(5): 376–386, 2010.
- [17] V. Arakelian, S. Sargsyan, On the design of serial manipulators with decoupled dynamics *Mechatronics*, 22: 904–909, 2012.